JOURNAL OF BACTERIOLOGY, May 2010, p. 2633–2637 Vol. 192, No. 10
0021-9193/10/$12.00 doi:10.1128/JB.00854-09

Repellent Taxis in Response to Nickel Ion Requires neither Ni^{2+} Transport nor the Periplasmic NikA Binding Protein▽

Derek L. Englert,[1] Christopher A. Adase,[2] Arul Jayaraman,[1,3] and Michael D. Manson[2,4]*

Artie McFerrin Department of Chemical Engineering,[1] Department of Biochemistry and Biophysics,[2] Department of Biomedical Engineering,[3] and Department of Biology,[4] Texas A&M University, College Station, Texas 77843

Received 29 June 2009/Accepted 15 January 2010

Ni^{2+} and Co^{2+} are sensed as repellents by the *Escherichia coli* Tar chemoreceptor. The periplasmic Ni^{2+} binding protein, NikA, has been suggested to sense Ni^{2+}. We show here that neither NikA nor the membrane-bound NikB and NikC proteins of the Ni^{2+} transport system are required for repellent taxis in response to Ni^{2+}.

Escherichia coli cells are repelled by Ni^{2+} and, with lower sensitivity, Co^{2+} (21). This response is mediated primarily by the aspartate/maltose chemoreceptor, Tar. A Tar-Tsr chimeric receptor fused at residues 256 and 257 of Tar still senses Ni^{2+}, whereas the reciprocal Tsr-Tar chimera does not (15). The authors of that study concluded that Ni^{2+} is sensed by the N-terminal periplasmic region of Tar. The fusion joint is actually near the C-terminal end of AS2, the second amphipathic helix of the HAMP domain (4) that couples the transmembrane sensing domain to the cytoplasmic kinase control domain. Thus, a more cautious interpretation of their results is that the ability to sense Ni^{2+} is conferred by the periplasmic, transmembrane, or HAMP region of Tar.

The five-gene *nikABCDE* operon encodes an ATP-dependent high-affinity uptake system for Ni^{2+}. This operon is quite similar in its construction to the five-gene operons encoding the oligopeptide (Opp) and dipeptide (Dpp) transport systems (2, 14). Furthermore, the periplasmic binding proteins encoded by the first gene of all three operons are very similar in their folds (23). The DppA protein interacts with the Tap chemoreceptor of *E. coli* and is the substrate recognition component of the attractant chemotaxis response to dipeptides (1, 8, 16).

The NikA binding protein (19) has been suggested to be the substrate recognition component of repellent chemotaxis to Ni^{2+} (7). However, there are several problems with this proposal. First, NikA is produced only under conditions of anaerobiosis (7) and Ni^{2+} limitation (6), but Ni^{2+} taxis is seen in cells grown aerobically in tryptone broth (18), whether or not $NiSO_4$ is present (9). Second, concentrations of Ni^{2+} that are needed to see significant responses to up or down step changes are between 10 and 100 μM (22), whereas the dissociation constant (K_d) for Ni^{2+} binding to NikA is on the order of 0.1 μM (7). Third, the other periplasmic binding proteins of *E. coli* that are involved in chemotaxis—DppA, the ribose-binding protein (RBP) (3), the galactose/glucose-binding protein (GBP) (13), and the maltose-binding protein (MBP) (12)—all mediate attractant taxis. Thus, NikA would have to evoke a response opposite from those generated by the other binding proteins.

These apparent discrepancies led us to examine whether NikA actually is the Ni^{2+} sensor in *E. coli*. We obtained knockout mutations of the *nikA*, *nikB*, and *nikC* genes from the Keio collection (5). These mutations replace the bulk of a given gene sequence with a kanamycin resistance cassette. The knockout mutations were transferred into the chemotactically wild-type strain CV1 (identical to RP437) (20), and the transfer of the mutations was confirmed by PCR analysis. To ensure that we were always working with mutant cells, we left the Kan^r cassettes in the disrupted genes. Although the *nikA* insertion could have a polar effect on *nikBCDE* and the *nikB* insertion could have a polar effect on *nikCDE*, we could still independently assess the effect of knocking out Ni^{2+} transport while retaining NikA with the *nikB* and *nikC* insertions and the effect of eliminating Ni^{2+} binding protein and transport with the *nikA* insertion.

The effects of the *nikA*, *nikB*, and *nikC* mutations on chemotaxis were assessed using our recently described microfluidic chemotaxis device (9). In this device, diffusive mixing between two inlet concentrations of a chemoeffector is used to generate a gradient of the chemoeffector. Bacteria entering the device immediately encounter the midpoint of the gradient and are exposed to it for 18 to 21 s before imaging. This assay allows easy and rapid quantification of the chemotactic response.

Figure 1 shows the response of wild-type and Δ*tar* and *nik* mutant cells to gradients of aspartate and $NiSO_4$. High-motility *E. coli* cells were prepared as described previously (9), except that cells were harvested and washed by centrifugation at 150 × *g* instead of by filtering. The low-speed centrifugation method produced a higher proportion of fully motile cells. Cells in chemotaxis buffer containing 50 μM L-aspartate or 122.5 μM $NiSO_4$ were introduced at the midpoint of 0 to 50 mM aspartate or 0 to 225 μM $NiSO_4$ gradients. CV1 cells give a very clear response in a 0 to 100 μM gradient of L-aspartate (Fig. 1A). CV1 cells also show a net migration toward lower concentrations of $NiSO_4$ (Fig. 1B). Cells of the isogenic Δ*tar* mutant CV4 show no response to the aspartate gradient, but they do seem to be repelled by higher $NiSO_4$ concentrations, although significantly less than CV1 cells.

* Corresponding author. Mailing address: Department of Biology, Texas A&M University, College Station, TX 77843. Phone: (979) 845-5158. Fax: (979) 845-2891. E-mail: mike@mail.bio.tamu.edu.

▽ Published ahead of print on 12 March 2010.

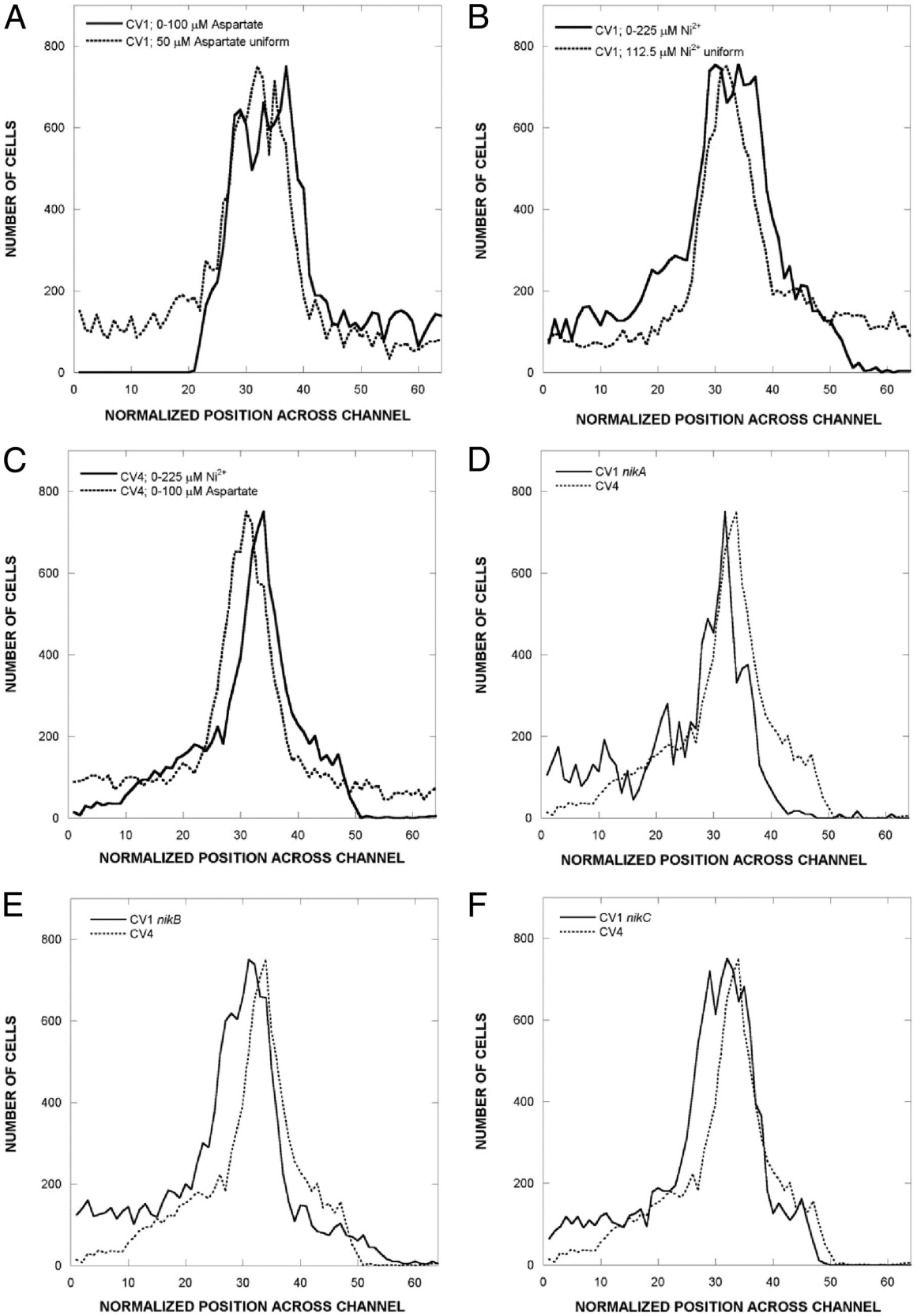

FIG. 1. Distribution of wild-type and *nik*-knockout strains in aspartate and $NiSO_4$ gradients. Cells were exposed to gradients in a previously described microfluidic device (9). The dimensions of the observation chamber are 20 by 1,050 by 11,500 μm. (A) Response of CV1 to a 0 to 100 μM gradient of L-aspartate. Cells were introduced in the middle of the channel in the presence of 50 μM aspartate. The distribution of cells at

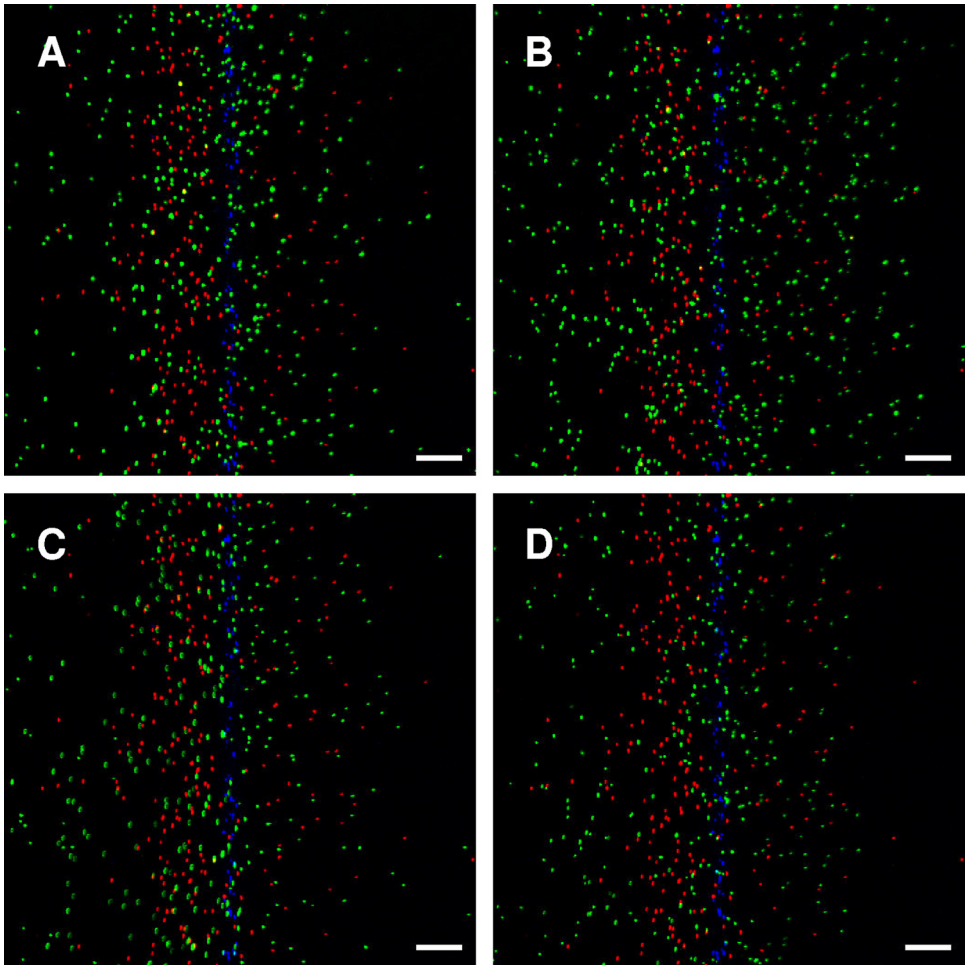

FIG. 2. Images of cells responding to a $NiSO_4$ gradient in the microfluidic device. CV1, CV4, and CV1 *nik*-knockout strains were exposed to a gradient of 0 to 225 μM $NiSO_4$. Representative pseudocolored overlay images are shown. The high concentration is at the right side of the image. In all images, CV1 or CV1 *nik*-knockout cells are shown in green, CV4 cells are shown in red, and dead cells are shown in blue. (A) CV1; (B) CV1 *nikA*; (C) CV1 *nikB*; (D) CV1 *nikC*. Note that some of the CV1, CV1 *nik*, and CV4 cells always go in the "wrong" direction, toward higher concentrations of $NiSO_4$. Readers are reminded that chemotaxis occurs via a biased random walk, so that on a short time scale (18 to 21 s) some cells will randomly go toward higher $NiSO_4$ concentrations. The scale bar is 100 μm.

The responses of CV1 *nik* mutant cells are shown in Fig. 1D to F. All three *nik* mutants show a net migration toward lower $NiSO_4$ concentrations comparable to that of strain CV1. Similar results were obtained when the flow rate was lower, but under those conditions the cells were exposed to the gradient for a longer time before imaging, and the average distance migrated was greater (data not shown). Pseudocolored images of the distribution of cells in $NiSO_4$ gradients are shown in Fig. 2. These photographs capture one instantaneous distribution, whereas the distributions shown in Fig. 1 are averaged over many images.

The extent of migration in response to the $NiSO_4$ gradient was quantified based on the chemotaxis partition and migration coefficients (CPC and CMC, respectively) (9, 17). The CPC value reflects the direction of migration (i.e., toward or away from a gradient) and quantifies the number of bacteria on either side of the bacterial inlet. For example, a CPC value of −0.30 indicates that 30% more bacteria move to the lower-

a uniform concentration of 50 μM aspartate is shown for comparison. (B) Responses of strain CV1 to a 0 to 225 mM gradient of $NiSO_4$. In the gradient, cells were introduced in the middle of the channel in the presence of 122.5 μM $NiSO_4$. The distribution of cells at a uniform concentration of 122.5 μM $NiSO_4$ is shown for comparison. (C) Distribution of CV4 (Δ*tar*) cells in gradients of 0 to 100 μM aspartate and 0 to 225 μM $NiSO_4$. Note that there is no significant attractant response to aspartate, but there is a residual repellent response to $NiSO_4$. (D) Responses of CV1 *nikA* and CV4 to a 0 to 225 μM gradient of $NiSO_4$. (E) Responses of CV1 *nikB* and CV4 to a 0 to 225 μM gradient of $NiSO_4$. (F) Responses of CV1 *nikC* and CV4 to a 0 to 225 μM gradient of $NiSO_4$. The same distribution for CV4 cells is shown in panels C to F. Cell counts for each were determined from 100 images taken over a 5-min interval from a point approximately 7 mm down the channel.

TABLE 1. Chemotaxis partition and migration coefficients in a $NiSO_4$ gradient[a]

Strain	Value for[b]:	
	CPC	CMC
CV1 (null gradient)	0.04 ± 0.01	0.04 ± 0.02
CV1	−0.31 ± 0.02	−0.13 ± 0.03
CV4	−0.08 ± 0.03	−0.06 ± 0.03
CV1 *nikA*	−0.25 ± 0.05	−0.11 ± 0.01
CV1 *nikB*	−0.39 ± 0.06	−0.16 ± 0.05
CV1 *nikC*	−0.26 ± 0.01	−0.11 ± 0.01

[a] The gradient ranged from 0 to 225 μM $NiSO_4$ in chemotaxis buffer across the 1,050-μm-wide channel, except for the null gradient, in which the $NiSO_4$ concentration was uniformly 122.5 μM across the channel.
[b] Values are means ± standard deviations, with $n \geq 3$.

concentration side than the higher-concentration side. The CMC weights the migration of cells by the distance they move. For example, a cell that moves to the left to the farthest low-concentration position (channel 1) is given a weighting factor of −1, whereas one that moves halfway into the lower concentration side (channel 16) is given a weighting factor of −0.5. CMC values are larger at lower flow rates.

The CPC values for CV1 and all three *nik* mutants (Table 1) were similar (−0.21 to −0.39). The CPC value for CV4 cells was −0.08. Cells in a null gradient of $NiSO_4$ (a uniform 122.5 μM across the channel width) showed a slight bias to the right (CPC of 0.04). Such small CPC values are probably not significant because of the difficulty in accurately estimating cell number near the point where they enter the chemotaxis channel (i.e., where the cell density is maximal). The CMC values were also comparable for the wild type and *nik* mutants (−0.11 to −0.16) and significantly higher than for the CV4 *tar* mutant in the same gradient (CMC of −0.06). The CMC value for CV1 cells in the null gradient was 0.05. These results show that repellent taxis in response to $NiSO_4$, even in this relatively shallow gradient, does not require NikA, NikB, or NikC. It should be noted that $NiSO_4$ at concentrations of up to 300 μM does not significantly inhibit growth or motility in tryptone broth (9).

Our results clearly show that Ni^{2+} taxis can occur in the absence of the Nik proteins. The marginal response of CV4 cells to the Ni^{2+} gradient raises the possibility that Ni^{2+} is sensed by chemoreceptors other than Tar. The response is so weak that it could have been missed in previous, less-sensitive assays. To test whether the other high-abundance chemoreceptor of *E. coli*, Tsr, is responsible for the residual $NiSO_4$ taxis, we assayed the responses of strains CV12 (Δ*tar* Δ*tap trg*::Tn*10*; Tsr as sole chemoreceptor) and CV13 (Δ*tsr* Δ*tap trg*::Tn*10*; Tsr as sole chemoreceptor) to a 0 to 122.5 μM $NiSO_4$ gradient. Strain CV12 failed to show any significant response, whereas strain CV13 gave a very robust response (Fig. 3).

An isothermal calorimetric (ITC) analysis shows unequivocally that Ni^{2+} binds specifically to the isolated periplasmic domain of Tar but not to the isolated periplasmic domain of Tsr (I. Kawagishi, personal communication). That conclusion is consistent with our observation that Ni^{2+} uptake is not required for repellent taxis in response to Ni^{2+}. The loss of Ni^{2+} sensing by Tar should give a sufficient difference in behavior to allow for an enrichment, using a variation of our recently developed microfluidic device (9), for *tar* mutants that are Ni^{2+} blind but still competent for maltose and/or aspartate taxis (10). In this way, we hope to characterize the Ni^{2+}-binding site in detail and shed more light on the poorly understood mechanism of repellent taxis.

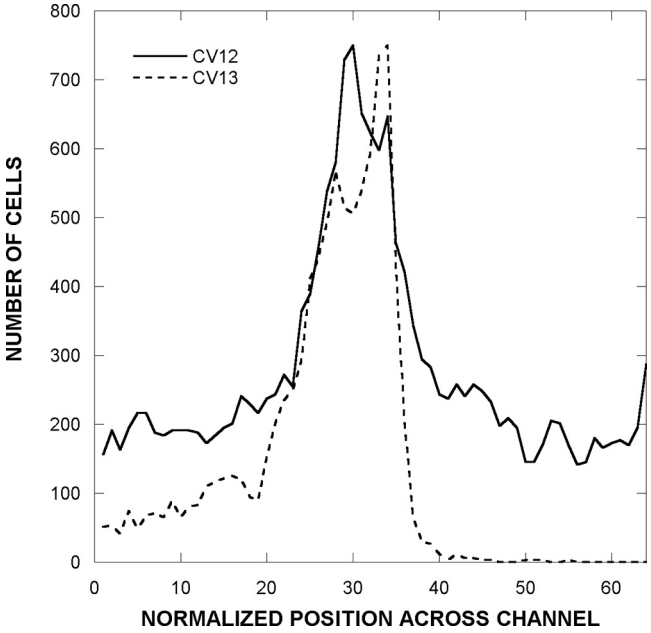

FIG. 3. Distribution of CV12 (Tsr only) and CV13 (Tar only) strains in a $NiSO_4$ gradient. The assay was run as described in the legend to Fig. 1.

We thank Ikuro Kawagishi for communicating results prior to publication. We are grateful for the Keio strains provided by the Genome Analysis Project and National BioResource Project (NIG, Japan): *E. coli*.

This work was supported by a grant from the National Science Foundation (CBET 0846453) to A.J. and by the Bartoszek Fund for Basic Biological Science to M.D.M.

REFERENCES

1. **Abouhamad, W. N., M. Manson, M. M. Gibson, and C. F. Higgins.** 1991. Peptide transport and chemotaxis in *Escherichia coli* and *Salmonella typhimurium*: characterization of the dipeptide permease (Dpp) and the dipeptide-binding protein. Mol. Microbiol. **5:**1035–1047.
2. **Abouhamad, W. N., and M. D. Manson.** 1994. The dipeptide permease of *Escherichia coli* closely resembles other bacterial transport systems and shows growth-phase-dependent expression. Mol. Microbiol. **14:**1077–1092.
3. **Aksamit, R. R., and D. E. Koshland, Jr.** 1974. Identification of the ribose binding protein as the receptor for ribose chemotaxis in *Salmonella typhimurium*. Biochemistry **13:**4473–4478.
4. **Aravind, L., and C. P. Ponting.** 1999. The cytoplasmic helical linker domain of receptor histidine kinase and methyl-accepting proteins is common to many prokaryotic signalling proteins. FEMS Microbiol. Lett. **176:**111–116.
5. **Baba, T., T. Ara, M. Hasegawa, Y. Takai, Y. Okumura, M. Baba, K. A. Datsenko, M. Tomita, B. L. Wanner, and H. Mori.** 2006. Construction of *Escherichia coli* K-12 in-frame, single-gene knockout mutants: the Keio collection. Mol. Syst. Biol. **2:**2006.0008.
6. **de Pina, K., V. Desjardin, M. A. Mandrand-Berthelot, G. Giordano, and L. F. Wu.** 1999. Isolation and characterization of the *nikR* gene encoding a nickel-responsive regulator in *Escherichia coli*. J. Bacteriol. **181:**670–674.
7. **de Pina, K., C. Navarro, L. McWalter, D. H. Boxer, N. C. Price, S. M. Kelly, M. A. Mandrand-Berthelot, and L. F. Wu.** 1995. Purification and characterization of the periplasmic nickel-binding protein NikA of *Escherichia coli* K12. Eur. J. Biochem. **227:**857–865.
8. **Dunten, P., and S. L. Mowbray.** 1995. Crystal structure of the dipeptide binding protein from *Escherichia coli* involved in active transport and chemotaxis. Protein Sci. **4:**2327–2334.
9. **Englert, D. L., M. D. Manson, and A. Jayaraman.** 2009. A flow-based

microfluidic device for quantifying bacterial chemotaxis in stable, competing gradients. Appl. Environ. Microbiol. **75:**4557–4564.
10. **Gardina, P., C. Conway, M. Kossmann, and M. Manson.** 1992. Aspartate and maltose-binding protein interact with adjacent sites in the Tar chemotactic signal transducer of *Escherichia coli*. J. Bacteriol. **174:**1528–1536.
11. Reference deleted.
12. **Hazelbauer, G. L.** 1975. Maltose chemoreceptor of *Escherichia coli*. J. Bacteriol. **122:**206–214.
13. **Hazelbauer, G. L., and J. Adler.** 1971. Role of the galactose binding protein in chemotaxis of *Escherichia coli* toward galactose. Nat. New Biol. **230:**101–104.
14. **Hiles, I. D., L. M. Powell, and C. F. Higgins.** 1986. Peptide transport in *Salmonella typhimurium*: molecular cloning and characterization of the oligopeptide permease genes. Mol. Gen. Genet. **206:**101–109.
15. **Krikos, A., M. P. Conley, A. Boyd, H. C. Berg, and M. I. Simon.** 1985. Chimeric chemosensory transducers of *Escherichia coli*. Proc. Natl. Acad. Sci. U. S. A. **82:**1326–1330.
16. **Manson, M. D., V. Blank, G. Brade, and C. F. Higgins.** 1986. Peptide chemotaxis in *E. coli* involves the Tap signal transducer and the dipeptide permease. Nature **321:**253–256.
17. **Mao, H., P. S. Cremer, and M. D. Manson.** 2003. A sensitive, versatile microfluidic assay for bacterial chemotaxis. Proc. Natl. Acad. Sci. U. S. A. **100:**5449–5454.
18. **Miller, J. H.** 1972. Experiments in molecular genetics. Cold Spring Harbor Laboratory Press, Cold Spring Harbor, NY.
19. **Navarro, C., L. F. Wu, and M. A. Mandrand-Berthelot.** 1993. The *nik* operon of *Escherichia coli* encodes a periplasmic binding-protein-dependent transport system for nickel. Mol. Microbiol. **9:**1181–1191.
20. **Parkinson, J. S., and S. E. Houts.** 1982. Isolation and behavior of *Escherichia coli* deletion mutants lacking chemotaxis functions. J. Bacteriol. **151:**106–113.
21. **Tso, W. W., and J. Adler.** 1974. Negative chemotaxis in *Escherichia coli*. J. Bacteriol. **118:**560–576.
22. **Ward, S. M., A. Delgado, R. P. Gunsalus, and M. D. Manson.** 2002. A NarX-Tar chimera mediates repellent chemotaxis to nitrate and nitrite. Mol. Microbiol. **44:**709–719.
23. **Wu, L. F., and M. A. Mandrand-Berthelot.** 1995. A family of homologous substrate-binding proteins with a broad range of substrate specificity and dissimilar biological functions. Biochimie **77:**744–750.

JOURNAL OF BACTERIOLOGY, Aug. 2010, p. 4259 Vol. 192, No. 16
0021-9193/10/$12.00 doi:10.1128/JB.00661-10

ERRATUM

Repellent Taxis in Response to Nickel Ion Requires Neither Ni^{2+} Transport nor the Periplasmic NikA Binding Protein

Derek L. Englert, Christopher A. Adase, Arul Jayaraman, and Michael D. Manson

Artie McFerrin Department of Chemical Engineering, Department of Biochemistry and Biophysics, Department of Biomedical Engineering, and Department of Biology, Texas A&M University, College Station, Texas 77843

Volume 192, no. 10, p. 2633–2637, 2010. Page 2633, right column, last paragraph: "0 to 50 mM aspartate" should read "0 to 100 μM aspartate."

Page 2635: The following should appear at the end of the legend to Fig. 1: The plots with dotted lines in Fig. 1D to F are the same as the plot with the solid line in Fig. 1C.

Page 2636, left column, next-to-last paragraph: "CV13 (Δ*tsr* Δ*tap trg*::Tn*10*; Tsr as sole chemoreceptor)" should read "CV13 (Δ*tsr* Δ*tap trg*::Tn*10*; Tar as sole chemoreceptor)."